Proc. Natl. Acad. Sci. USA
Vol. 85, pp. 2974–2978, May 1988
Biophysics

Ca^{2+}-activated synexin forms highly selective, voltage-gated Ca^{2+} channels in phosphatidylserine bilayer membranes

(acidic phospholipids/membrane reconstitution)

HARVEY B. POLLARD AND EDUARDO ROJAS

Laboratory of Cell Biology and Genetics, National Institutes of Health, Bethesda, MD 20892

Communicated by Bernhard Witkop, November 10, 1987

ABSTRACT **Synexin, a cytosolic protein that mediates Ca^{2+}-dependent membrane fusion, was incorporated into acidic phospholipid bilayers, formed at the tip of a patch pipet. The pipet was filled with a high-Ca^{2+} solution (50 mM) and immersed in a chamber containing a low-Ca^{2+} solution (1 mM). Brief exposures of the bilayer to synexin increased the capacitance of the bilayer by a factor of 10 and decreased the membrane resistance by a factor of 20. Reduction of Ca^{2+} in the chamber to 1 μM caused an abrupt increase in the current required to hold the pipet potential at 0 mV. Under certain conditions channel events could be detected, often occurring in bursts. Consistently, open-time histograms were found to be voltage-dependent and to exhibit one time constant in the time range examined here. The slope conductance for the synexin channel was estimated as 10.2 ± 2.1 pS for the large Ca^{2+} gradient with low chamber Ca^{2+}. However, for symmetrical, low-Cl^- solutions containing 25 mM Ca^{2+} the conductance was 26.5 ± 5.2 pS. Ion-replacement studies showed the synexin channel to much prefer Ca^{2+} over Ba^{2+} or Mg^{2+}. Cd^{2+}, a potent blocker of other voltage-gated Ca^{2+} channels at 100 μM, blocked synexin channels only at very high concentrations (≥10 mM). Similarly, nifedipine, an inhibitor of the nonactivating Ca^{2+} channel, was effective only at extremely high concentrations (>300 μM). The high selectivity for Ca^{2+} and the lack of response of the channel to various drugs known to block Ca^{2+} channels thus distinguish the synexin channel from other types of Ca^{2+} channels hitherto reported.**

Fusion of membranes is a fundamental event underlying exocytosis and many other biological processes (1). In the case of exocytosis from adrenal medullary chromaffin cells, fusion between secretory vesicles and between secretory vesicles and plasma membranes depends on increased intracellular Ca^{2+} concentration (2) and may be mediated by intracellular Ca^{2+}-binding proteins such as synexin (3–5). Synexin is a compelling candidate for such a mediator because of its affinity for the relevant membranes and its fusion properties *in vitro*. For example, Ca^{2+}-activated synexin binds to both chromaffin granules and the inner aspect of chromaffin-cell plasma membranes (6). Synexin also mediates chromaffin-granule aggregation (3) and fusion (7, 8), fusion of chromaffin-granule ghosts (9), and fusion of liposomes prepared from acidic phospholipids such as phosphatidylserine (PtdSer) (10, 11). Further, the fusion structures generated from native chromaffin granules faithfully resemble the compound exocytotic structures seen by electron microscopy in secreting chromaffin cells (12). Therefore, we and others have concluded that an accurate understanding of the molecular mechanism of synexin action might lead to fundamental insights into the fusion processes occurring during exocytosis *in vivo*.

The publication costs of this article were defrayed in part by page charge payment. This article must therefore be hereby marked "*advertisement*" in accordance with 18 U.S.C. §1734 solely to indicate this fact.

At least part of the mechanism of synexin action could involve an intimate association of the molecule with the membrane to be fused. In support of this concept is our recent work showing that Ca^{2+}-activated synexin can penetrate into the low-dielectric core of a PtdSer bilayer (13, 14). These data, as well as other evidence for the strong hydrophobic character of Ca^{2+}-activated synexin, led us to propose that synexin might promote fusion by acting as a hydrophobic bridge, spanning the fusing membranes and allowing the otherwise parallel lipid bilayers to cross and mix (14).

Inasmuch as the hydrophobic-bridge hypothesis predicts that synexin could enter into and perhaps span the membrane, it occurred to us that synexin might also exhibit channel activity. Such activity would then provide unambiguous evidence that synexin could indeed enter and span the membrane as well as provide strong support for our interpretation of earlier studies of synexin-induced membrane-capacitance increases. We found, as described in this paper, that synexin indeed forms channels and that the channel is highly selective for Ca^{2+}. We also found that the pH optimum and the action of phenothiazine drugs (15) on the channel were as expected from the biochemistry of synexin. We conclude that synexin channels are quite different from the three other types of Ca^{2+} channels found in many cells (16) and that our concept of fusion involving penetration of synexin molecules into the substance of the bilayer may be valid.

MATERIALS AND METHODS

Electrical Measurements. Pipets were prepared from microhematocrit capillary tubes (i.d. 1.1–1.2 mm; wall thickness 0.2 mm) by use of a programmable microelectrode puller (BB-CH, Mecanex, Geneva). These pipets had a total capacitance of 3–10 pF, the lower value being for pipets coated almost to the tip with Sylgard, as described by Sakmann and Neher (17). The open tip resistance ranged from 5 to 20.0 MΩ, and when bilayers were prepared by the double-dip method (18) the resistance rose to 1–3 GΩ.

Membrane currents under voltage-clamp conditions were recorded with a List amplifier (EPC-7, List Electronics). The amplifier was used without compensation for the series resistance and with the capacity null-bridge turned off. Current signals were fed through a low-pass filter (8-pole Bessel, model 902-LPF, Frequency Devices, Haverhill, MA) with the corner frequency set at 10 kHz to the input amplifier of an analog magnetic tape recorder (Racal Recorders, Sarasota, FL).

Solutions. Solutions used inside the patch pipets were filtered (Millex-GV, 0.22-μm pore size, Millipore). The glass chamber, having a total volume of 0.3 cm^3, contained a buffer solution with either 1 mM or 1 μM Ca^{2+}. The composition of the solutions used on either side of the bilayer are described in *Results*. PtdSer monolayers were spread by direct application of PtdSer to the surface (1 cm^2)

Abbreviation: PtdSer, phosphatidylserine.

of the chamber from a glass rod, following evaporation of the solvent (chloroform) from the rod.

Purification of Synexin. Highly purified synexin was prepared from bovine liver by a method involving ammonium sulfate fractionation, chromatography on Ultrogel (LKB) (3), and purification to near homogeneity by chromatofocusing (19). The protein was stored at −20°C in a lyophilized state until use. To verify purity synexin was subjected to $NaDodSO_4$/15% PAGE according to Laemmli (20) and stained with either Coomassie blue G-250 or silver. To assess proteolysis, aliquots were subjected to immunoblot analysis using either monoclonal or polyclonal antibodies to synexin. Only highly pure, unproteolyzed samples were used, and the results here were obtained with two different batches of synexin that were prepared separately.

Chemicals. PtdSer (Avanti Polar Lipids, Birmingham, AL) was dissolved in chloroform (0.1 mg/ml) and kept at −70°C. All aqueous solutions were Millipore-filtered before use. All glassware was washed with Milli-Q water, ethanol, and chloroform before use. All solutions were prepared with Milli-Q water. All reagents and solutions were tested for channel-forming properties.

RESULTS

PtdSer Bilayers on a Patch Pipet. To study the details of the interactions of synexin with membranes made from acidic phospholipids, we prepared bilayers composed of PtdSer, an acidic phospholipid for which synexin has Ca^{2+}-dependent affinity (14). These bilayers were formed by a double-dip method (18) using pipets filled with a buffer (pH 7.4) containing 50 mM Ca^{2+}. Other solutions with less Ca^{2+} were also suitable. Before the formation of the bilayer, a typical pipet had an open-tip resistance of 10 MΩ, while after formation of the bilayer the resistance increased to 1–3 GΩ. Measurements of displacement currents (13) revealed that the capacitance of these bilayers was close to 20 fF, as expected for a bilayer formed at the tip of a patch pipet with an open tip 1 μm in diameter. Furthermore, application of voltage pulses exceeding 450 mV always broke the membrane, suggesting dielectric breakdown of the bilayer (21).

Channel Formation by Synexin in PtdSer Bilayers. Another patch pipet was used to deliver controlled amounts of synexin to the bilayer. By application of rectangular pulses of pressure inside the pipet containing synexin (pneumatic PPM-2 unit, Neuro Phore, BH-2 system, Medical Systems, Great Neck, NY), a stream of a synexin solution (6 $\mu g/cm^3$) could be directed towards the side of the bilayer facing the solution in the chamber. To get optimal incorporation of synexin into the bilayer, the "puffing" of the protein was carried out at pH_i 6.5 and $[Ca^{2+}]_i$ adjusted to 1 mM. (In this model system, the chamber solution corresponds to the intracellular compartment; hence, chamber Ca^{2+} concentration and pH are denoted $[Ca^{2+}]_i$ and pH_i, and Ca^{2+} concentration and pH in the pipet are $[Ca^{2+}]_o$ and pH_o.) Synexin incorporation was also assayed at different $[Ca^{2+}]_i$ (0.1–2 mM) and pH_i (6–7.4) values. Provided the pH_i was <7, incorporation of synexin was also observed at lower $[Ca^{2+}]_i$ (0.1 mM). However, with either lower $[Ca^{2+}]_i$ or higher pH_i the incorporation was less efficient. Under the conditions routinely used for the incorporation of synexin (i.e., $[Ca^{2+}]_i$ equal to 1 mM and pH_i adjusted to 6.5), the membrane current across the bilayer was low, thereby making it possible to measure membrane capacitance from the charge displaced during and after voltage-clamp pulses. The charge was calculated by integration of the current transients as described (13, 14). As a rule, after exposure of the bilayer to synexin the current was always "noisier" than in control records obtained before the application of the protein.

Once synexin was incorporated into the membrane, we adjusted $[Ca^{2+}]_i$ to <1 μM by adding EGTA (3.3 mM) to the solution in the chamber. The immediate consequence of lowering $[Ca^{2+}]_i$ was a dramatic increase in the holding current, to values as high as −250 pA. In all experiments reported here, the flow of current corresponded to the movement of positive charge in the direction of the chemical gradient for Ca^{2+}. Numerous abrupt current jumps between discrete levels were observed, suggesting the presence of a large number of active channels in the bilayer. To reduce the number of active channels, we used specific inhibitors (22). In the case of synexin-induced membrane-conductance increase, we resorted to the phenothiazine inhibitors trifluoperazine and promethazine (15). Alternatively, we simply lowered the synexin concentration, a strategy we employed to obtain our analytical data.

While studying the effects of phenothiazine drugs on synexin-channel formation, we learned that addition of as little as 5 μM trifluoperazine to the solution in the chamber precluded observation of channel activity upon addition of synexin. However, additions of trifluoperazine (30–100 μM) to the solution in the chamber *after* establishment of increased membrane capacitance and membrane conductance allowed us to clearly observe single-channel currents (Fig. 1). The magnitude of the unitary event was 2.6 ± 0.2 pA at a pipet potential of 30 mV, meaning that before blockade by trifluoperazine the bilayer contained about 100 active channels. On a bilayer of 1-μm^2 area this would correspond to 100 channels per μm^2. We found that promethazine was somewhat less potent than trifluoperazine but still able to block conductance of PtdSer bilayers with incorporated synexin. These data thus indicated that the channels conduct Ca^{2+} down the electrochemical gradient. Furthermore, phenothiazine drugs, effective blockers of the aggregation and fusion properties of synexin as well as of secretion from intact cells (15), not only prevented channel formation but also were effective blockers of the channel activity. Under conditions where unitary events could be readily observed, we noted that channel openings (or closings) tended to occur in bursts (Fig. 1). Each burst was separated by a longer period in which the channel remained shut (or open). Heated synexin (30 min at 100°C) was inactive in forming channels, as expected from the inactivity of heated synexin in all previous biochemical tests.

Electrical Characteristics of Synexin Channels in Absence of Drugs. Fig. 2 shows the responses of a PtdSer bilayer with incorporated synexin to rectangular voltage pulses, taking the pipet potential from the holding level of 0 mV to −30 mV (*Left*, top record) and to 30 mV (*Right*, top record). No phenothiazine drugs were present and details of the synexin-channel activity are shown below the records on an expanded time base. From records like those shown in Fig. 2,

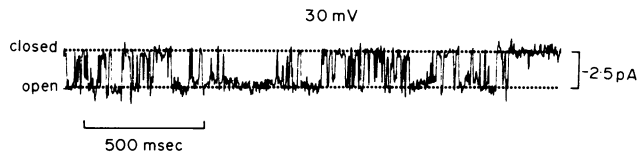

FIG. 1. Single synexin-channel currents. In the presence of <1 mM Ca^{2+} in the chamber, the pipet potential was held at various levels from −60 to 60 mV for 3-min periods. Although recording of the holding current at high gain (20 or 50 mV/pA) revealed that the current was larger for negative than for positive pipet potentials, there was no indication of channel activity in the records. Thus, this control rules out the possibility of the presence of channel-forming contaminants in our experimental solutions, including the phospholipid solution. The solution in the chamber contained 3 mM EGTA and $[Ca^{2+}]_i$ was estimated as 1 μM. The trifluoperazine concentration was 100 μM. The pipet was filled with a 50 mM Ca^{2+} solution and the record was made at a pipet potential of 30 mV. The mean value of the current was −2.5 pA, and the low-pass filter was set at 1 kHz.

we then measured the size of the events and constructed amplitude distribution histograms at various pipet potentials.

As exemplified in Fig. 3*B*, amplitude histograms had normal distribution, indicating the presence of a population of synexin channels with a single conductance level and the absence of conductance substrates for the channel. The mean values from six individual histograms have been plotted as a function of pipet potentials in Fig. 3*A*. The straight line was drawn to fit the points with a slope representing the single-channel conductance equal to 10.2 ± 2.1 pS. The intercept on the potential axis occurs at −205 mV, in reasonable agreement with the Nernst potential of −159 mV calculated on the basis of the $[Ca^{2+}]$ gradient ($[Ca^{2+}]_o/[Ca^{2+}]_i = 5 \times 10^4$). Reassuringly, in symmetrical, Cl^--free solutions (25 mM Ca^{2+} on each side of the bilayer), the reversal potential of the current was zero, as expected.

Kinetic Properties of Synexin Channels. From records like those in Fig. 2 we also measured the time intervals between channel opening (distribution of closed times) and between channel closings (distribution of open times). Open-time and closed-time histograms (10-msec bin width) clearly required more than one time constant to fit the points. The time scale used for the histograms shown in Fig. 4, although adequate to separate the different time constants (17), was selected to illustrate that the kinetics are affected by the electric field across the membrane. Table 1 summarizes the results. It may be seen that the time constant depended on pipet potential, indicating that the open-channel probability was voltage-dependent.

Ionic and Pharmacologic Selectivity of Synexin Channels. We analyzed the ion selectivity of synexin channels by replacing K^+ with tetraethylammonium and using tetramethylammonium/Pipes and Tris/Hepes as pH buffers (instead of Na Pipes and Na Hepes). Under these conditions, negative single-channel currents (−2.2 pA at a pipet potential of 20 mV) were recorded. To distinguish Ca^{2+} current from Cl^- current we used sodium isethionate in place of KCl but maintained the $CaCl_2$ concentration constant. Isethionate is quite impermeant for a variety of Cl^- channels, including those of chromaffin granules (23). Again, this substitution had no effect on either the amplitude of the single-channel current or the frequency of appearance of the events.

Focusing then on other divalent cations, we tested Ba^{2+} and Mg^{2+}. We found that with Ba^{2+} (50 mM) in the pipet, bilayer formation was virtually impossible unless Ca^{2+} (2 mM) was also present in the solution in the chamber. Under these conditions, synexin could be incorporated into the PtdSer bilayer, as evidenced by our ability to drive Ca^{2+} from the bath into the pipet. However, after $[Ca^{2+}]_i$ was lowered from 2 mM to 1 μM by the addition of EGTA to the solution in the chamber, there was no indication of channel activity. This result thus demonstrates the high selectivity for Ca^{2+} of the synexin channel in PtdSer bilayers. Consistently, addition of $BaCl_2$ (50 mM) to the solution in the chamber during the recording of synexin single-channel activity (50 mM $CaCl_2$ in the pipet) did not profoundly interfere with Ca^{2+} current. To verify that Ca^{2+} current was

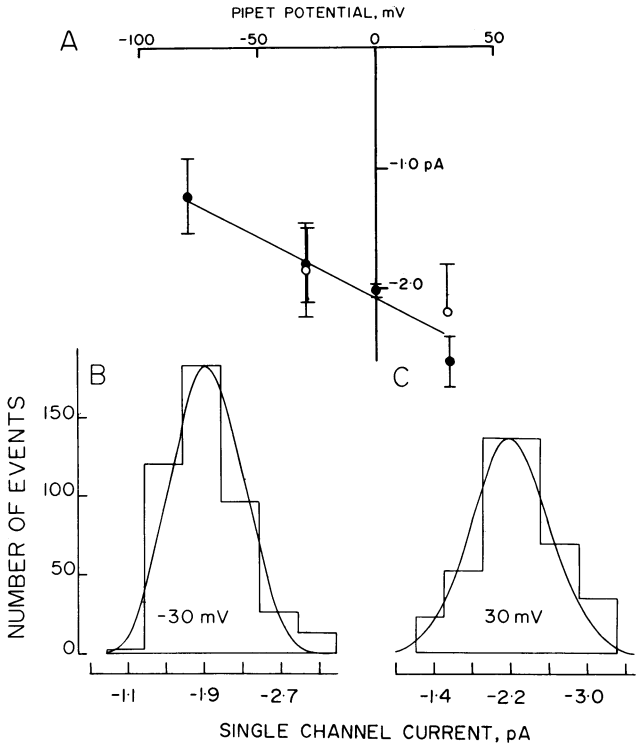

FIG. 3. Current–voltage relationship for the open synexin channel and amplitude histograms. (*A*) The fitted line corresponds to $I_{Ca} = \gamma V_p + I^0_{Ca}$, where γ is the single-channel conductance (10 pS) and I^0_{Ca} is the intercept [i.e., the value of the current at 0 mV pipet potential V_p (−2.09 pA)]. The reversal potential for the single-channel current was obtained from the extrapolated intercept on the V_p axis (not shown), −205 mV. Open circles correspond to the mean values for the histograms shown in *B* and *C*. Filled circles are data similar to that in *B* and *C*, but at different values of pipet potential. Error bars represent twice the SD. For each distribution of channel-current amplitudes, the fitted line corresponds to $dV_p/dI = 1/(2\pi)^{0.5}\exp[-(I - \langle I\rangle)^2/2\sigma^2]$. (*B*) Amplitude histogram for V_p = −30 mV. Parameters used for the fit: $\langle I\rangle$ = −1.86 pA and σ = 0.4 pA. (*C*) Amplitude histogram for V_p = 30 mV. Parameters used for the fit: $\langle I\rangle$ = −2.2 pA and σ = 0.4 pA.

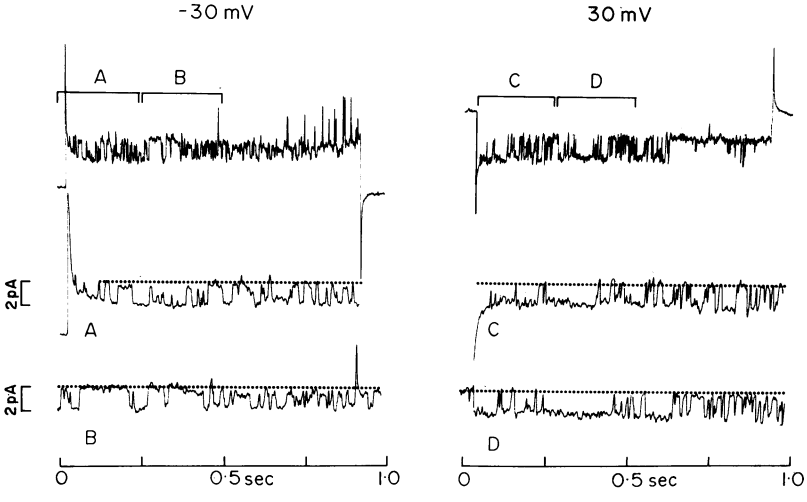

FIG. 2. Voltage dependence of synexin-channel openings. (*Left*) Upper record shows the response to a rectangular voltage pulse taking the pipet potential from 0 to −30 mV. Channel events on expanded time base are shown below (A and B). Dotted line is the closed state. (*Right*) Upper record was obtained in response to the application of a rectangular voltage pulse taking the pipet potential from 0 to 30 mV. Segments of this record (C and D) are shown below on an expanded time base. Dotted line is the closed state.

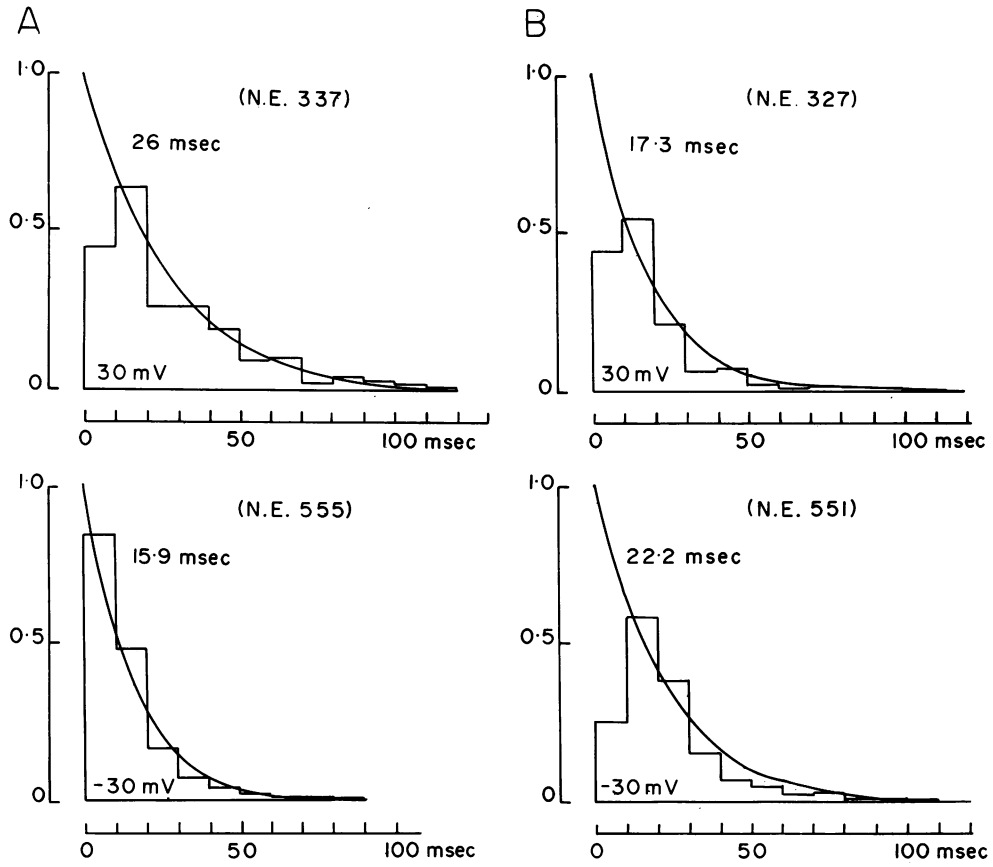

FIG. 4. Open-time and closed-time distributions. Single-channel recordings from synexin voltage-gated ion channels were obtained at 12 different pipet potentials, ranging from −80 to 30 mV. The data base used for the open-time and closed-time distributions corresponds to recordings with a signal/noise ratio ≥3:1. All events of duration <0.2 msec have been discarded. Such event omission introduces a small distortion of the observed channel kinetics. Number of events (N.E.) for the data base associated with each histogram is given in parentheses. The minimum number of open states entered by the synexin channel can be estimated by determining the number of exponential components needed to fit the observed open-time distribution (17). For each histogram the fitted line corresponds to $f_o = \Sigma(\alpha_i/\tau_i)\exp(-t/\tau_i)$, where i represents the number of states and f_o represents open-state event frequency. For this time scale only one time constant τ was required. τ values are given next to the corresponding fitted curves. (*A*) Open-time distributions. Time constants were obtained from plots of the number of events (on logarithmic scale) as a function of the open time for each distribution. (*B*) Closed-time distributions. Time constants were obtained as in *A*.

conducted through the open synexin channel in the direction of the electrochemical gradient, we reversed the $[Ca^{2+}]$ gradient. Under these conditions, positive single-channel currents were recorded, demonstrating that Ca^{2+} moves through the open channel down its electrochemical gradient. Furthermore, addition of either Ba^{2+} or Mg^{2+} to the solution in the chamber caused no noticeable changes in the characteristics of the single-channel currents described before. These data indicate that with this specific protocol synexin does not interact with Ba^{2+} or Mg^{2+}, vastly preferring Ca^{2+} as an ionic substrate. These properties are coincident with previously known biochemical properties of synexin and therefore are not particularly surprising.

Inasmuch as the synexin channel seemed so different from other Ca^{2+} channels in terms of divalent-cation specificity, we also examined the effects of other specific and nonspecific Ca^{2+} channel inhibitors. Cd^{2+} and nifedipine, at concentrations known to block voltage-gated Ca^{2+} channels (100 μM Cd^{2+}) or noninactivating Ca^{2+} channels (1 μM nifedipine), had little effect on synexin-channel activity. However, Cd^{2+} at 10 mM reduced synexin-dependent Ca^{2+} current, while nifedipine became inhibitory only at 300 μM.

Table 1. Time constants (τ) from synexin-channel open- and closed-time histograms

	τ, msec			
Histogram	−30 mV	10 mV	20 mV	30 mV
Open time	16	9	16	26
Closed time	20	13	8	17

Recordings were made at pipet potentials of −30, 10, 20, and 30 mV. Data base for each histogram ranged from 300 to 480 events. Time constants were obtained as explained in the legend to Fig. 4.

DISCUSSION

Ca^{2+}-activated synexin molecules were found to spontaneously form Ca^{2+} channels in PtdSer bilayers. One important aspect of this finding is that it verifies that Ca^{2+}-activated synexin can actually insert into the low-dielectric region of the bilayer. This is consistent with our previous conclusion, based on changes in capacitance of these bilayers induced by Ca^{2+}-activated synexin (13). These findings and conclusions are also consistent with the mechanistic details of our recent hypothesis explaining membrane fusion (14). According to this hypothesis, Ca^{2+}-activated synexin protrudes simultaneously into the core of both fusing membranes, creating a hydrophobic bridge over which lipids cross and mix together. This point of contact is inherently unstable and a macroscopic channel communicating the two compartments is generated.

The concept of a folded, water-soluble protein being able to enter a membrane and form channels upon appropriate activation is, of course, not unique to synexin. In fact, a variety of water-soluble proteins can enter membranes and form relatively nonselective, voltage-gated ion channels. These include diphtheria toxin B (24), colicin Ia (25), botulinum and tetanus toxin (26), and complement (27). Other

widely appreciated forms of protein movement into and across membranes have included the cotranslational insertion mechanisms involving hydrophobic leader sequences (28). However, there have been increasing numbers of reports showing posttranslational membrane insertion of proteins, not even associated with leader sequences (29). We therefore conclude that there is ample mechanistic precedent for the insertion of native, water-soluble synexin molecules into the membrane, perhaps driven by a conformational transition that emphasizes a hydrophobic character on the protein surface. Synexin is certainly different, but only in the sense of the exquisite selectivity of the channel.

An important consideration in evaluating these data is the extent to which we are convinced that the channels we studied were indeed formed by synexin and not by some contaminant present in very low concentrations in the pure synexin preparation. However, the most compelling evidence favoring the identity of the channels with synexin is the unusual, synexin-like property of the synexin channels themselves. In fact, as shown in *Results*, synexin-channel properties are virtually identical to the Ca^{2+}-dependent granule-aggregation properties of synexin but are quite unlike those of all other previously described Ca^{2+} channels.

For example, synexin channels are specific for Ca^{2+}, being nonselective for Ba^{2+} or Mg^{2+} under our assay conditions. This is exactly the case for both synexin-dependent granule aggregation (3) and synexin polymerization (4). By contrast, Ca^{2+} channels from plasma membranes (30) or from transverse-tubule membrane (31) conduct Ba^{2+} with greater or at least equal efficiency than they do Ca^{2+}. In fact, synexin is the only Ca^{2+} channel yet reported that conducts Ba^{2+} so poorly.

An additional point of similarity between synexin-channel activity and synexin-dependent granule aggregation is the sensitivity of the two processes to low concentrations of both trifluoperazine and promethazine. Except as inhibitors of synexin (15) and of secretion (15, 32, 33), where they are effective in low micromolar concentrations, these two phenothiazine drugs are at opposite ends of the activity spectrum. Medically, trifluoperazine (Stelazine) is a good antischizophrenia drug, whereas promethazine (Compazine) is good only to treat nausea. Trifluoperazine is a good local anesthetic and inhibitor of calmodulin, whereas promethazine is about 0.01 times as potent (15).

Finally, two typical inhibitors of Ca^{2+} channels, Cd^{2+} (30) and nifedipine (34), are relatively less effective as inhibitors both of synexin channels and of other biochemical properties of synexin. Cd^{2+} at 2 mM, a concentration 20-fold higher than that required to block the T-type Ca^{2+} channels (16), affects synexin channels only marginally. The more sensitive L- and N-type Ca^{2+} channels are blocked by 10 μM Cd^{2+} (16). Thus, synexin forms the only Ca^{2+} channel yet reported that is so insensitive to Cd^{2+}. The ineffectiveness of the dihydropyridines is less instructive, however, since T- and N-type channels are also not sensitive to them. The preponderance of the data therefore leads us to the conclusion that if the channel activity in our synexin preparation were indeed due to a "contaminant," then the membrane aggregation and fusion properties of the synexin preparation would have to be due to the same contaminant. We conclude that the 47-kDa synexin molecule is likely to be the material basis of the aggregation and fusion activity as well as the channel activity.

These data could also lead to a reappraisal of the increasingly popular technique of following exocytosis by measuring increases in capacitance of the secreting cell. For example, in both chromaffin (35) and mast (36, 37) cells, stimulation of exocytosis is accompanied by increases in membrane capacitance. While it is certainly true that membrane addition (increase in area of the plasma membrane) can raise the capacitance, these increases could also be due to additional dipoles in the membrane causing measurable increases in the dielectric constant. Such dipoles could include synexin or synexin-like molecules (14).

We thank Dr. A. Lee Burns for his continuous material and intellectual contributions to this work and Ms. Diana Johnson-Seaton for preparation of synexin.

1. Alberts, B., Bray, D., Lewis, J., Raff, M., Roberts, K. & Watson, J. D. (1983) *Molecular Biology of the Cell* (Garland, New York).
2. Pollard, H. B., Ornberg, R., Levine, M., Kelner, K., Morita, K., Levine, R., Forsberg, E., Brocklehurst, K. W., Duong, L., Lelkes, P., Heldman, E. & Youdim, M. (1985) *Vitam. Horm. (N.Y.)* **42**, 109–196.
3. Creutz, C. E., Pazoles, C. J. & Pollard, H. B. (1978) *J. Biol. Chem.* **253**, 2858–2866.
4. Creutz, C. E., Pazoles, C. J. & Pollard, H. B. (1979) *J. Biol. Chem.* **254**, 553–558.
5. Morris, S. J., Hughes, J. M. & Whittaker, V. P. (1982) *J. Neurochem.* **39**, 529–536.
6. Scott, J. H., Creutz, C. E., Pollard, H. B. & Ornberg, R. (1985) *FEBS Lett.* **180**, 17–23.
7. Creutz, C. E. (1981) *J. Cell Biol.* **91**, 247–256.
8. Creutz, C. E. & Pollard, H. B. (1982) *Biophys. J.* **37**, 119–120.
9. Stutzin, A. (1986) *FEBS Lett.* **197**, 274–280.
10. Hong, K., Duzgunes, N. & Papahadjopoulos, D. (1981) *J. Biol. Chem.* **256**, 3641–3644.
11. Hong, K., Duzgunes, N. & Papahadjopoulos, D. (1982) *Biophys. J.* **37**, 297–305.
12. Pollard, H. B., Creutz, C. E., Fowler, V. M., Scott, J. H. & Pazoles, C. J. (1982) *Cold Spring Harbor Symp. Quant. Biol.* **46**, 819–833.
13. Rojas, E. & Pollard, H. B. (1987) *FEBS Lett.* **217**, 25–31.
14. Pollard, H. B., Rojas, E. & Burns, A. L. (1987) *Ann. N.Y. Acad. Sci.* **493**, 524–541.
15. Pollard, H. B., Scott, J. H. & Creutz, C. E. (1983) *Biochem. Biophys. Res. Commun.* **113**, 908–915.
16. Miller, R. J. (1987) *Science* **235**, 46–52.
17. Sakmann, B. & Neher, E. (1983) *Single Channel Recording* (Plenum, New York).
18. Suarez-Isla, B. A., Wan, K., Lindstrom, J. & Montal, M. (1983) *Biochemistry* **22**, 2319–2323.
19. Scott, J. H., Kelner, K. L. & Pollard, H. B. (1985) *Anal. Biochem.* **149**, 163–165.
20. Laemmli, U. K. (1970) *Nature (London)* **227**, 680–685.
21. Benz, R. & Conti, F. (1981) *Biochim. Biophys. Acta* **645**, 115–123.
22. French, R. J., Kruege, B. K. & Worley, J. F., III (1986) in *Ionic Channels in Cells and Model Systems*, ed. Latorre, R. (Plenum, New York), pp. 273–288.
23. Pazoles, C. J., Creutz, C. E. & Pollard, H. B. (1980) *J. Biol. Chem.* **255**, 7863–7869.
24. Kagan, B. L., Finkelstein, A. & Colombini, M. (1981) *Proc. Natl. Acad. Sci. USA* **78**, 4950–4954.
25. Raymond, L., Slatin, S. L. & Finkelstein, A. (1985) *J. Membr. Biol.* **84**, 173–181.
26. Hoch, D. H., Romero-Mira, M., Ehrlich, B. E., Finkelstein, A., Das Gupta, B. R. & Simpson, L. L. (1985) *Proc. Natl. Acad. Sci. USA* **82**, 1692–1696.
27. Young, J. D.-E., Cohn, Z. A. & Podack, E. R. (1986) *Science*, **233**, 184–190.
28. Wickner, W. T. & Lodish, H. F. (1985) *Science* **230**, 400–407.
29. Zimmerman, R. & Mayer, D. I. (1986) *Trends Biochem. Sci.* **11**, 512–515.
30. Hagiwara, S. & Byerly, L. (1981) *Annu. Rev. Neurosci.* **4**, 69–125.
31. Hidalgo, J., Luxoro, M. & Rojas, E. (1979) *J. Physiol. (London)* **288**, 313–330.
32. Sussman, K. E., Pollard, H. B., Leitner, J. W., Nesher, R., Adler, J. & Cerasi, E. (1983) *Biochem. J.* **214**, 225–230.
33. Clapham, D. E. & Neher, E. (1984) *J. Physiol. (London)* **353**, 541–564.
34. Nayler, W. G. & Horowitz, J. D. (1983) *Pharmacol. Ther. Part B* **20**, 203–225.
35. Neher, N. & Marty, A. (1982) *Proc. Natl. Acad. Sci. USA* **79**, 6712–6716.
36. Zimmerberg, J., Curran, M., Cohen, F. S. & Brodwick, M. (1987) *Proc. Natl. Acad. Sci. USA* **84**, 1585–1589.
37. Almers, W. & Neher, E. (1987) *J. Physiol. (London)* **386**, 205–217.